ORNL

OAK RIDGE NATIONAL LABORATORY
OPERATED BY
UNION CARBIDE CORPORATION
NUCLEAR DIVISION
POST OFFICE BOX X
OAK RIDGE, TENNESSEE 37830

~~For Internal Use Only~~

ORNL
CENTRAL FILES NUMBER
68 - 11 - 20

DATE ISSUED: MAR 28 1969

DATE: November 19, 1968

COPY NO. 104

SUBJECT: Measurements of Fission-Product Deposition in the MSRE with Ge(Li) Gamma Ray Spectroscopy

TO: Distribution

FROM: R. Blumberg, F. F. Dyer, T. H. Mauney and Dunlap Scott

ABSTRACT

Measurements of fission products deposited in the piping, the heat exchanger, the pump bowl and the offgas system of the Molten-Salt Reactor Experiment (MSRE) were made by gamma-ray spectroscopy, following the shutdown of a long period of power operation. The remote maintenance shield and remote handling techniques were used because of high radiation coming from the shutdown reactor. A highly collimated, lithium-drifted germanium diode detector was coupled to a 400 channel analyzer to produce the energy spectra that constituted the basic measurements. These measurements were converted to area deposition concentrations for each isotope found, expressed in curies per square inch of metal surface. Ten isotopes were identified, with 5 being predominant in the heat exchanger. The results are tabulated for all the experimental data, summarized and compared to calculations of total amount of each isotope produced by the reactor. It appears that gamma ray spectroscopy is a useful technique for investigating fission product behavior in the MSRE.

NOTICE This document contains information of a preliminary nature and was prepared primarily for internal use at the Oak Ridge National Laboratory. It is subject to revision or correction and therefore does not represent a final report. The information is only for official use and no release to the public shall be made without the approval of the Legal and Information Control Department of Union Carbide Corporation, Nuclear Division.

CONTENTS

Measurements of Fission-Product Deposition in the MSRE with Ge(Li) Gamma Ray Spectroscopy

Purpose of Experiment

In molten-salt reactors, fission products deposit in components contacted by the fuel salt and the gases above the fuel salt. The types and amounts of fission products that deposit are important to the Molten Salt Reactor Program (MSRP) because of the heat they generate after reactor shutdown and because of their influence on remote maintenance of the reactor. A knowledge of the distributions of deposited fission products is of interest to determine if they are correlated with (1) fission-product precursor half lives, (2) thermal gradients within reactor components, and (3) molten-salt chemistry. In addition there is a specific interest in the extent of deposition of ^{95}Zr. All the Zr^{95} is expected to remain in the salt as the fluoride. The presence of appreciable ^{95}Zr in the heat exchanger could indicate that ZrO2 had precipitated on the tubes. This would lead to concern about the analyses of the oxygen concentration in the salt and corrosion of the reactor equipment. An effort was therefore made to identify and quantitatively estimate the amount of gamma-emitting fission products that deposit in various components (principally the heat exchanger) of the MSRE.

This is an extension of a previous effort made at the MSRE,[1] during the May 1967 shutdown. An ion chamber with a collimator was used to measure gross gamma activity and a NaI crystal detector with collimator was aimed at areas of the heat exchanger to obtain gamma-energy spectra. Information from the latter experiment led to the present work.

Experimental Method and Equipment

Measurements of fission product distributions were made at the MSRE, shortly after the cessation of a six month period of power operation, by gamma-ray spectroscopy using a highly collimated lithium-drifted germanium diode detector (GeLi). The detector had a resolution of 6 kev for the 1.33 Mev line of ^{60}Co. A low-noise detector preamplifier was coupled to a biased amplifier which was coupled to a 400-channel analyzer. The biased amplifier permitted spectra to be accumulated over an energy range encompassing the fission-product gamma energies (nominally about 100 to 900 kev). Several spectra were taken to include energies to about 2000 kev. Gamma spectra were recorded on punched paper tape for subsequent data reduction.

The configuration of the detector and collimator positioned over the heat exchanger is shown in Figure 1. The collimator consisted of a lead cylinder with a length and diameter of 32 1/2 and 19 in., respectively. The diode, in a small Dewar filled with liquid nitrogen, was placed in a cavity in the shield over a hole with a diameter and length of $\sim$0.125 in. and 12 in., respectively. The collimator permitted the detector to be "focused" on an area about 3 in. in diameter at a distance of 15 ft

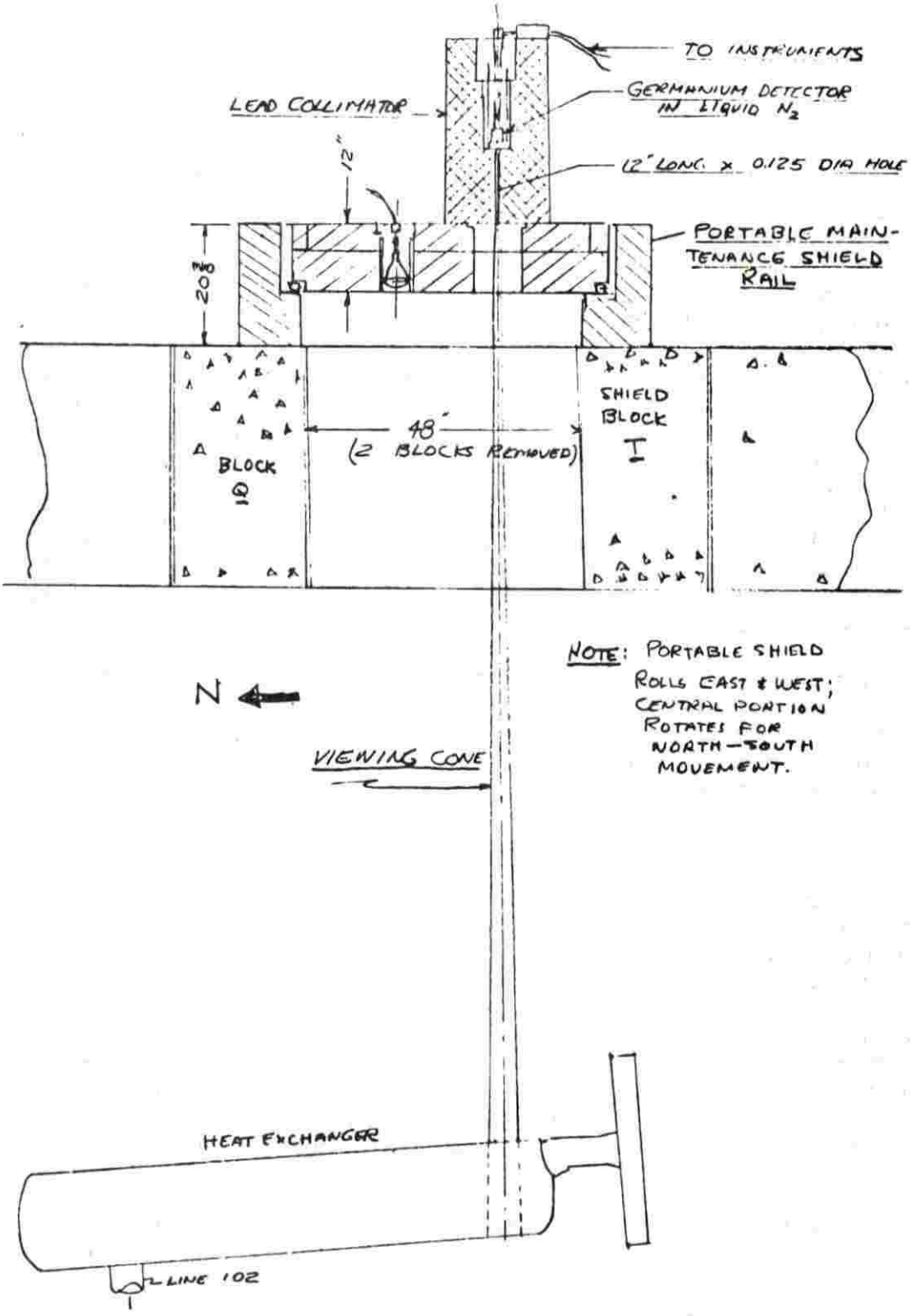

Fig. 1. Scanning System Sketch.

Table I. Chronology of the Measurements

Spectra No.	Time Elapsed Since Shutdown (hr)	Location *	Equipment and Condition
1 thru 19	486.0 92	R&F	Inlet end of heat exchanger – flush salt and coolant salt circulating; heater in place.
20 thru 29	114 118	R&S	Inlet end of heat exchanger – flush salt and coolant salt drained (heat exchanger empty; heater removed.
30 thru 39	138 142	Q&R	Middle of heat exchanger – no salt; heater removed.
34&39	140	Q&R	Line 102 – no salt; heater in place.
50 thru 66	227 324	G&H	Pump bowl – no salt.
53&54	229	G&H	Line 101 – no salt.
67 thru 89	325	G&H	Line 522 – no salt; jumper in place.
70 thru 89	345 353	Q&R	Middle of heat exchanger – no salt; no heater.
90 thru 99	356 360	S&T	Inlet end of heat exchanger and downstream end of Line 101 – no salt; heater in place.

*Letters refer to the lower shield blocks removed for access.

(distance to the heat exchanger). The detector-collimator assembly was mounted on and shielded by the portable maintenance shield which also served to move the detector to various positions over the reactor components.

The time spent in taking the data was scheduled in between reactor operations and various remote maintenance activities. Further, access to the reactor components was limited to the 4-ft-wide areas made available by the portable maintenance shield. Figures 2 and 3 show the reactor components examined and Table I gives the chronological sequence of the measurements, the reactor component, and the absorber situation. In summary, 67 usable spectra of the heat exchanger, the fuel pump, the off-gas line and primary system piping were taken during the period from 3 1/2 to 12 days after shutdown.

Fission Products Detected and Data Reduction

The fission products detected in the MSRE components, the energies and abundances (branching ratios) of their principal gamma rays are listed in Table II.

Table II. Nuclide Data

Nuclide	Energy (kev)	Abundance (%)	Half Life
^{95}Nb	765	100	35.0 days
^{99}Mo	740	12	66.7 hr
^{103}Ru	497	88	39.5 days
^{106}Ru	512	21	368 days
^{132}Te	230	95	77.7 hr
^{132}I	668	118	2.26 hr
^{132}I	773	89	2.26 hr
^{140}Ba	537	34	12.8 days
^{140}La	1596	109	40.2 hr
^{137}Cs	662	85	30.0 yr
^{141}Ce	145	48	32.5 days
^{131}I	364	82	8.05 days

A typical gamma-ray spectrum is shown in Figure 4. The spectrum was obtained six days after reactor shutdown with the detector centered over the heat exchanger 1 ft from the heat exchanger inlet. Full energy peaks (photopeaks) for several of the fission products found in the reactor components are indicated in Figure 4.

For quantitative calculations, it was necessary to obtain the net count rate, CR, under the full energy peaks for the various radionuclides detected. The method used to obtain CR is illustrated in Figure 4 for the 497 kev peak of ^{103}Ru. The gross count in a peak was determined by summing the counts per channel over the peak. The Compton base line (background) was calculated by multiplying the number of counts in the last

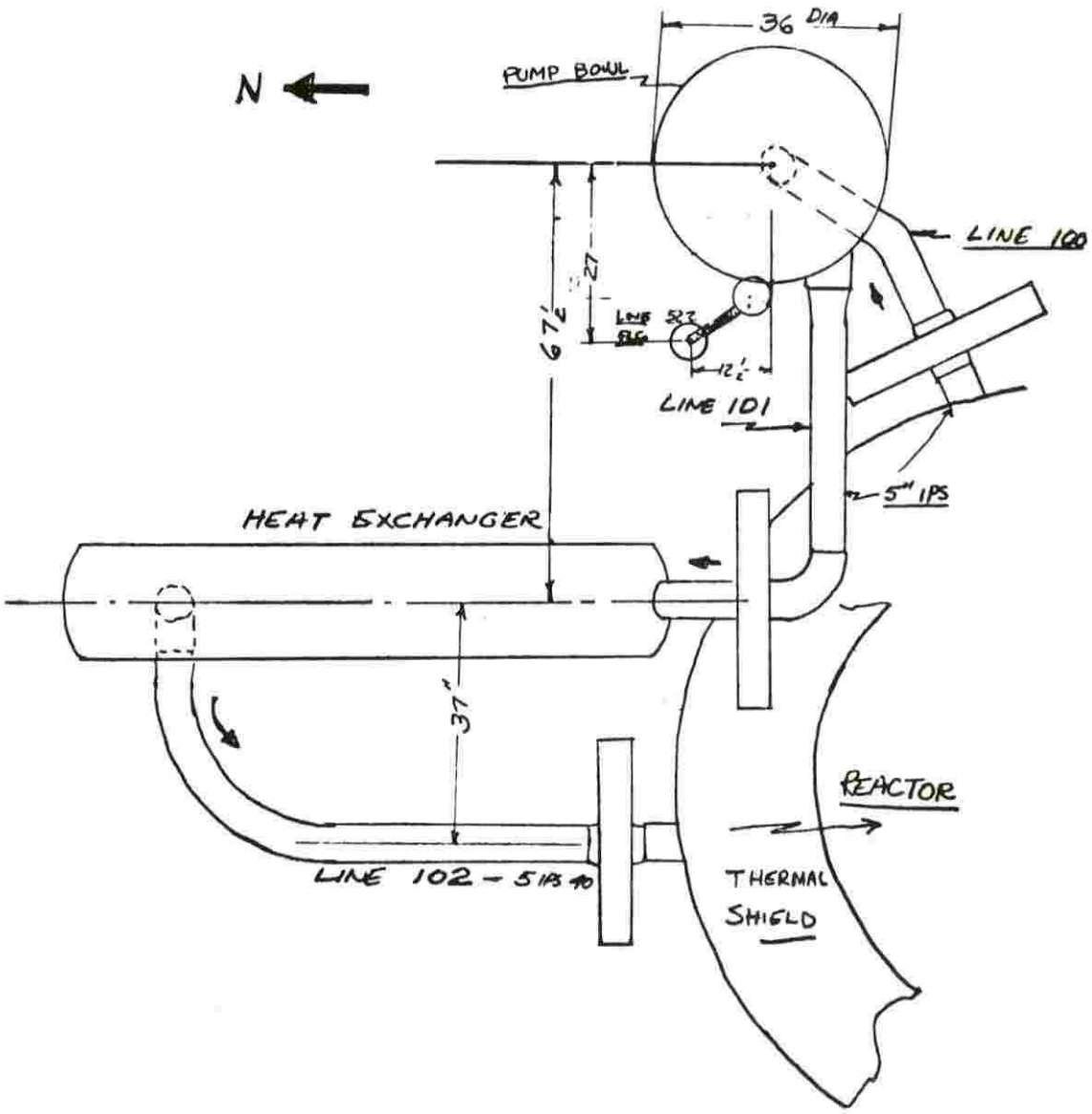

Fig. 2. Plan View of Items Scanned.

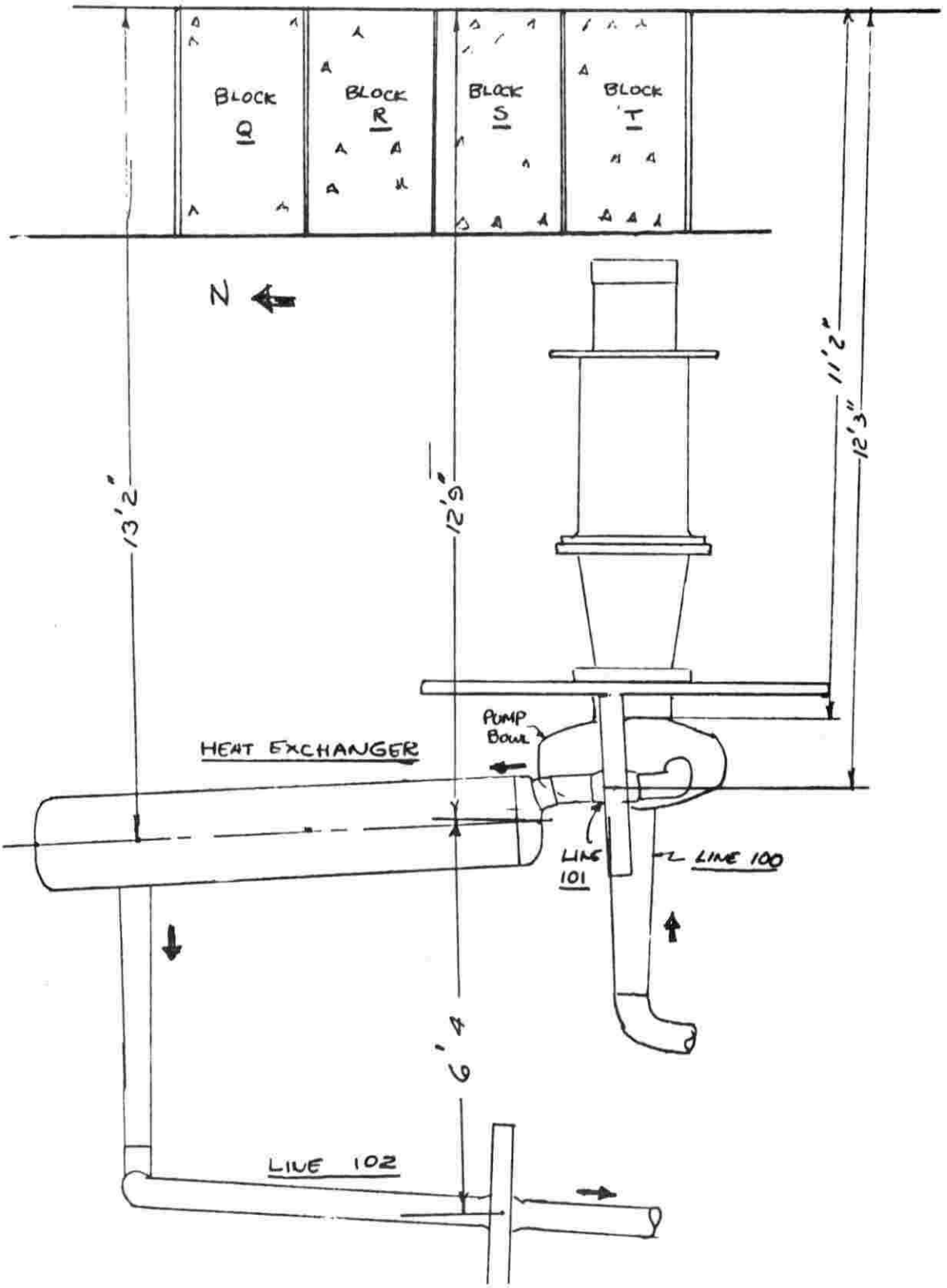

Fig. 3. Elevation Sketch of Heat Exchanger Line 102 and Pump.

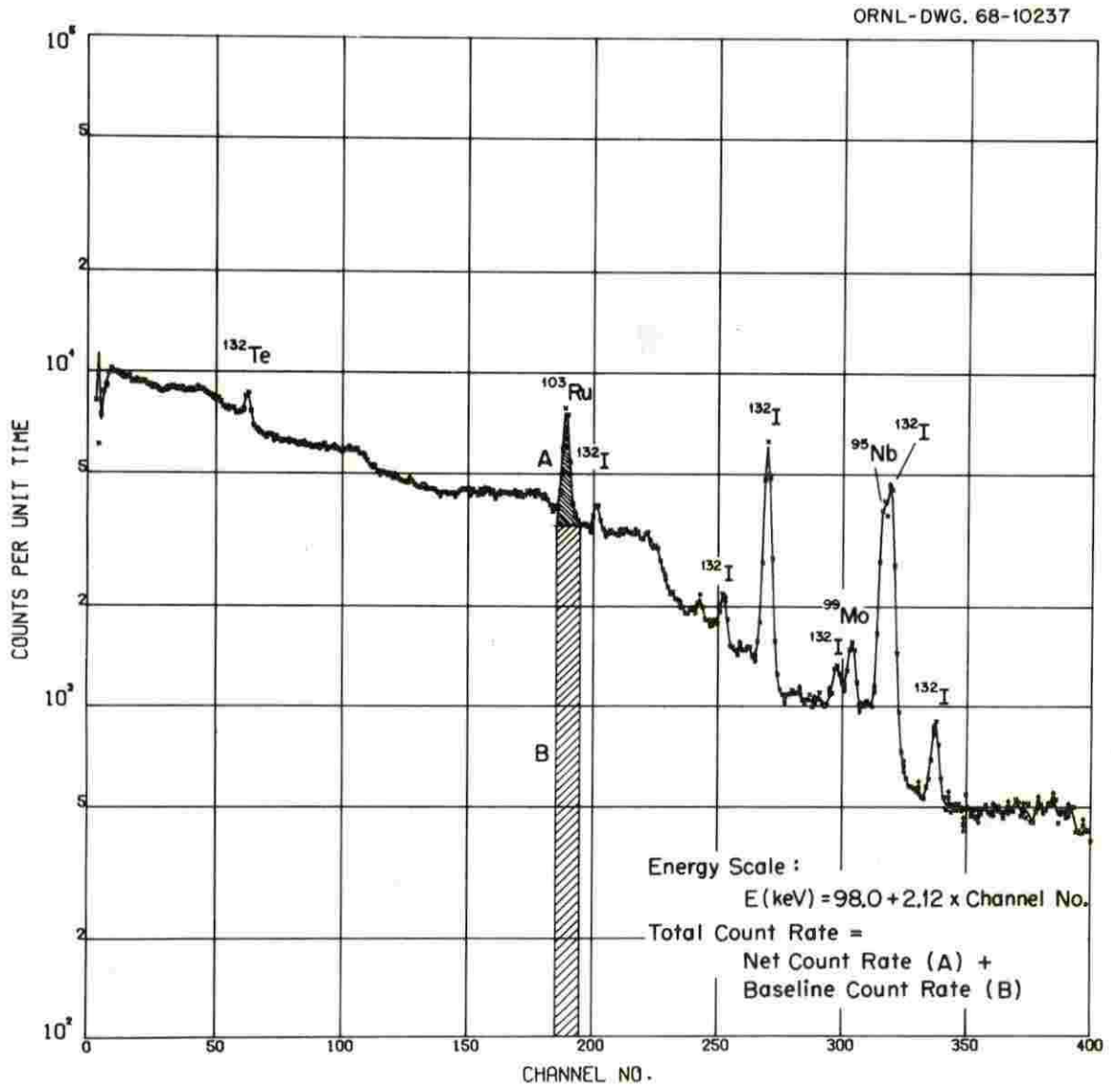

Fig. 4. Typical Spectrum.

channel (upper energy channel) taken for the peak, by the number of channels summed. The net count rate was then calculated by dividing the difference of the gross count and the base line by the counting time in seconds. To obtain the curies of a radionuclide deposited per square inch, CURIES, the following relation was assumed:

$$\frac{\text{CURIES}}{\text{in.}^2} = \frac{(\text{CR})e^{0.693t/T_{1/2}}}{(\text{F})(\text{B})(\text{AF})(\text{AB})\ 3.7 \times 10^{10}}, \qquad (1)$$

where t is the decay time in hours from reactor shutdown to the measurement time, $T_{1/2}$ is the half-life in hours of the specified radionuclide, B is the branching ratio of the measured gamma ray (photons emitted per disintegration), F is the counting efficiency, AF (area factor) is the number of square inches of metal surface with deposited isotopes per square inch of area normal to the axis of the detector, AB is an absorber factor denoting the fraction of the gamma photons that escape from the reactor component in the direction of the detector, and the factor 3.7×10^{10} converts the result to curies. The derivation of the counting efficiencies and the absorber factors are described in Appendix I.

Discussion of the Accuracy of the Results

The significance of the work done in this experiment is its value as design information for predicting the behavior of fission products in future molten salt reactors. With this in mind a discussion follows which attempts to estimate the accuracy of the results with regard to both the identification of the isotope and the amounts of deposited material.

We are certain that the correct identification of the isotopes has been made. The following discussion is in regard to the accuracy of the amounts reported. From Eq. (1) on p. 9 we see that the measured quantity, CR, (the count rate in counts per second) is modified by five factors. Of these, three are fairly well-known numerical values and therefore should introduce little error. These are: the decay factor, the branching ratio, and the area factor.

Larger inaccuracies, however, may appear in the two remaining factors, the absorber factor and the efficiency factor. There are three comparisons that can be made which lend a qualitative feeling of confidence to these results. One can compare results for different source-absorber configurations. One can compare the results of these measurements with calculations of the total inventory of each isotope produced in the power operation of the MSRE and finally one can compare these results with results of the chemical analysis of core and pump bowl samples. These comparisons are easily made, as in Table III, but one cannot point to a definite measure of accuracy.

TABLE III

Comparison of Gamma Measurements, Total Inventory Calculations, and Chemical Analysis of Core Samples

Isotope	Total Produced Curies/in.^{2} (1)	Gamma Measurement Curies/in.^{2} (2)	(3)	Analytical Chemistry Core-Samples Curies/in.^{2} (4)
95-Nb				
High		3.09	2.23	0.31
Low		0.95	0.69	0.10
Average	3.28	1.90	1.37	0.25
99-Mo				
High		9.20	6.78	0.79
Low		0.53	0.39	0.33
Average	4.78	4.88	3.69	0.612
103-Ru				
High		2.43	2.43	0.035
Low		0.19	0.19	0.025
Average	1.75	1.12	1.12	0.030
132-I				
High		6.17	4.81	
Low		0.51	0.70	
Average	3.32	2.18	1.70	
132-Te				
High		3.93	7.16	0.242
Low		0.46	0.84	0.175
Average	3.32	1.54	2.81	0.209

(1) Based on E. L. Compere's unpublished calculation of the inventory of each isotope at shutdown, divided by the total area of salt contacted metal surface of the primary system, provided by R. E. Thoma.

(2) As calculated with original efficiency curve given in Figure 5.

(3) As calculated with a revised efficiency curve.

(4) Results of data from core samples removed from MSRE, April 1968, Reported by Kirslis? et al.

One additional aspect concerning accuracy is involved in the criteria that all of the peaks from a multi-energy emitter such as ^{132}I, which appear on a spectra should yield the same result. Results from ^{132}I gamma rays at .668, .955 and 1.400 Mev revealed a discrepancy of a factor of 2. To satisfy the criteria one can change either the absorber factor, the efficiency factor or both. Since the adjustment was easier to accomplish and easier to rationalize, we chose to examine the effect of changing the efficiency factor. The two counting efficiency curves are shown in Figure 5. The new curve is not as steep as the one derived from the calibration data, and it has the effect of decreasing the results of isotopes with energies above .500 Mev and increasing results of isotopes with energies below .500 Mev. This effect increases the credibility of the present set of results. This effect is given only in the third data column of Table III. The results given throughout the report reflect the original efficiency factor. The correction is mentioned to give an indication of a possible source of inaccuracy.

In summary, one can conclude that these results can be inaccurate by as much as 200%.

Results and Conclusions

A summary of the results is given in Table IV. A complete list of raw data and calculated results is given in Appendix 2. Results for the examination of the heat exchanger, plotted in the plan view for each isotope, also appear in Appendix 2.

There was no ^{95}Zr found.

The pump bowl contains large concentrations of deposited isotopes although the values in Table V in Appendix II are probably high, due to uncertainties in the knowledge of the geometry of the site examined. It is interesting to note that the peak values for different isotopes do not occur at the same physical locations.

In the heat exchanger, five isotopes of 4 decay chains were found to predominate, ^{95}Nb, ^{99}Mo, ^{103}Ru, and ^{132}Te and I. The density of deposited fission products is generally higher at the exchanger inlet than further downstream, although it is not uniform. The term splotchy would be descriptive.

In Table III the fission product concentrations on the tubes in the heat exchanger, obtained from our measurements, are in very poor agreement with those obtained from analysis of deposits on specimens from the core. However, calculations reported in MSR 68-138[3] indicate that the mass transfer coefficients in the heat exchanger are probably a factor of 3 to 4 higher than in the vicinity of the samples in the core. Multiplying the results for the core samples by 4 brings them to within a factor of about 2 of our average results.

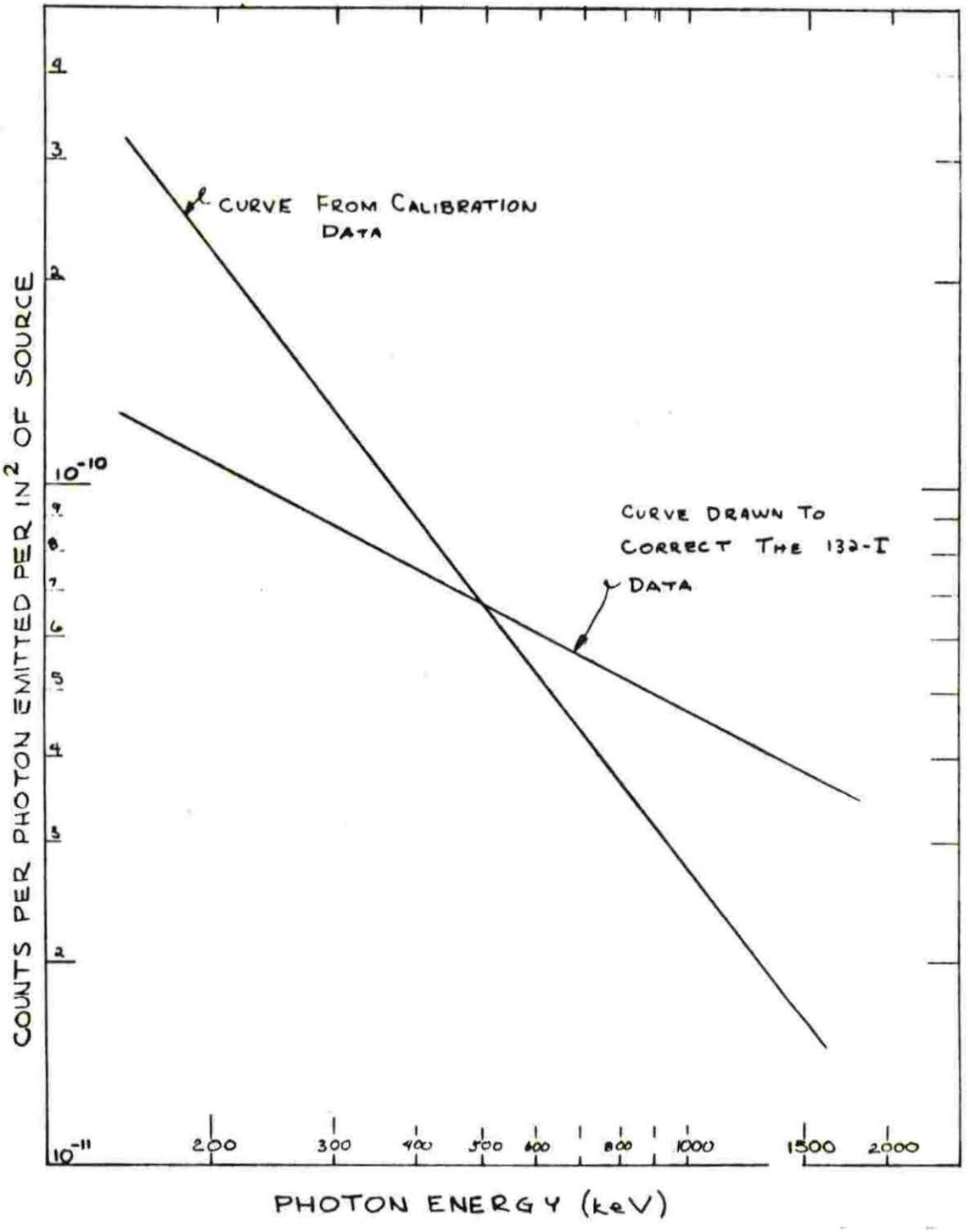

Fig. 5. Counting Efficiency vs Energy.

TABLE IV

Summary of Calculated Results (Curies/sq. in.)

Isotope	Heat Exchanger			Pump Bowl		Offgas Line	
	High	Low	Average	High(1)	Low	High	Low
95-Nb	3.09	0.95	1.90	1.36(50)	0.38	0.34	0.25
99-Mo	9.20	0.53	4.88	5.93(62)	22.99	36.24	28.61
103-Ru	2.43	0.19	1.12	35.97(62)	9.76	11.19	8.93
106-Ru				8.53(65)	1.51	1.83	1.48
131-I						1.29	0.95
132-I	6.17	0.51	2.18	0.78(62)			
132-Te	3.93	0.46	1.54	4.16(64)	4.16	--	--
137-Cs						2.57	2.24
140-La	0.047	0.011	0.028	0.78(66)	0.78	3.28	0.10
141-Ce						0.33	0.33

(1) The number in parentheses refers to locations shown in Figure 13.

There is an unexplained variation in the observed deposition of ^{132}I and its precursor Te in the heat exchanger. With flush salt in the system, these two fission products appear to be close to the proper relationship. With the flush salt drained, however, I is higher than Te by a factor of 1.5. This can be due either to a mechanism which causes higher concentration of I in the heat exchanger, or inaccuracies in the energy dependent factors used to calculate results from the raw data. Because its 230 kev energy peak is obscured by the background count, ^{132}Te does not appear on heat exchanger scans taken after the 14 days of decay (spectra 70 and on). However, its presence is known by the fact that ^{132}I is still detected. Further, consistent results for ^{132}I are calculated on the basis of the half life of the Te precursor, rather than the much shorter half life of the I itself.

In view of the fact that we are reasonably sure that we can improve accuracy and the ease of making the gamma measurements, one may conclude that gamma spectroscopy is a useful technique in fission product deposition studies.

Recommendations

Should this experiment be repeated, considerable improvement can be achieved. The following list of recommendations will increase confidence in the accuracy of the results, provide calculated results two to three days after taking the data, and increase the ease of operation for the experimenters.

1. Re-calibrate the equipment with a multi-energy gamma source.

2. Obtain an empirical value for the attenuation factor. This can be combined with item 1 above or conducted separately.

3. Modify the collimator, its mounting, and the method of establishing its position with respect to reactor components.

4. Set up all variables, inputs and computer programs so that the data can be analyzed quickly. This may require extra manpower during the data taking period.

5. Select and use the best possible detector and electronic components.

These recommendations will be described and discussed in more detail in a separate memorandum.

References

1. Molten Salt Reactor Program Semiann. Progress Report for Period Ending Aug. 31, 1967, ORNL-4191, pp 40-44.

2. Reactor Chemistry Division Semiann. Progress Report, not published.

3. R. B. Briggs, Estimate of the Afterheat by Decay of Noble Metals in MSBR and Comparison with Data from the MSRE, Nov. 4, 1968, MSR-68-138.

APPENDIX I

Detector Calibration

To permit quantitative estimation of the fission products, the collimated detector was calibrated with sources of known specific activity. In all measurements the source-to-detector distance was 15 ft. Because the reactor components, as measured by the detector, approximated plane sources, it was necessary to calibrate the detector with plane sources. Ideally, the calibrating source should be a thin plane slightly wider than the area subtended by the collimator. The source should contain one or more uniformly dispersed radionuclides which emit several gamma rays with energies spanning the gamma-energy range of the fission products. Because of several practical problems met in procuring such a source, a slightly modified procedure was used. A thin copper foil uniformly activated with neutrons to produce approximately 60 curies of ^{63}Cu was used to obtain a calibration point at 511 kev (the energy of annihilation photons). The foil was sandwiched between two 0.02-in. copper foils and measured. The photon emission rate per $in.^2$ of foil was standardized by measuring a specimen of known size cut from the foil on a NaI(Tl) scintillation detector calibrated by Heaths'[1] method. To obtain the counting efficiency as a function of energy, measurements were made with a small wafer (1/2 in. x 1/2 in. x 1/32 in.) containing about 30 curies of ^{192}Ir. Iridium-192 emits seven principal gamma rays with energies ranging from 296 to 612 kev. Because the ^{192}Ir was not a plane source, gamma spectra were taken with the source placed at several positions with respect to the center line of the collimator. For each spectrum, the net count rates for the full energy peaks were obtained and divided by the corresponding branching ratios. This permitted arbitrary efficiency curves to be plotted for each source position. All curves closely approximated straight lines but had slightly different slopes. The variation of slope with source placement is thought to be due to the collimator edge which causes increasing attenuation with decreasing gamma energy. Each curve was normalized to the absolute efficiency value derived at 511 kev with ^{64}Cu. A median line drawn through the curves was used to obtain counting efficiencies for calculations with Eq. (1). The median line differed from the measured efficiency lines having maximum and minimum slopes by about ±11% at 230 kev (gamma energy of ^{132}Te) and ±5% at 765 kev. The efficiency curve is shown in Figure 5.

Net Count Rates of ^{95}Nb

Because of the relatively poor resolution of the detector, the 765 kev gamma rays of ^{95}Nb were not resolved from the 773 kev gamma rays of ^{132}I and 780 kev gamma rays of ^{99}Mo. The resulting broad full-energy peak is indicated in Figure 4. To obtain the net count rate for ^{95}Nb, it was necessary to subtract from the total net counts in the peak the counts due to ^{132}I and ^{99}Mo. The total net count rate was calculated as previously described. Because the 668 kev gamma ray of ^{132}I and the 740 kev gamma ray of ^{99}Mo were resolved, it was possible to use Eq. (1) and thus calculate

the net count rate under the unresolved peaks from the net count rates under the resolved peaks. For ^{132}I the expression used was

$$CR_{773} = CR_{668} \frac{B_{773}F_{773}(AB)_{773}}{B_{668}F_{668}(AB)_{668}} \qquad (2)$$

Method of Calculation of Absorber Factors

It is desired to calculate the fraction of those gamma rays, emitted from isotopes uniformly deposited on the metal tubes of the heat exchanger, which penetrate the absorber material between it and the detector. The penetrating rays, S, coming from a point source S_o, through absorber material whose coefficient of attenuation, and thickness are μ and t is given by

$$S = S_o e^{-\mu t}$$

The total source from N points is $NS = S_o \sum_{i=1}^{N} e^{-\mu t_i}$

and

$$\frac{NS}{NS_o} = \frac{\sum_{i=1}^{N} e^{-\mu t i}}{N},$$

which is the ratio of the penetrating rays divided by the rays which are emitted. We call this ratio the absorber factor. We chose N so that the area considered is typical of the geometry so that the ratio given does not change for different locations or larger areas.

Thus the calculation involves the surface on which source material is deposited and the thicknesses of absorber material. In this experiment the different geometries that were encountered are shown in Figure 6. For most of the heat exchanger cases the absorber material consists of metal tube walls and the vessel's shell, while other cases also involve the heat exchanger heater and the flush salt. As shown in Figure 7, the area of deposition; i.e., the outside of the tube is divided into equal segments of area. In the calculationa a quadrant was divided into 18 areas. Corresponding to these are values of tube thickness ("y" in the sketch) and flush and coolant salt thickness (the dotted lines in the sketch). These absorber lengths were generated graphically. Note that radiation from source Q travels through tubes in two vertical columns while radiation from source P travels through tubes in only one vertical column. This fact complicates the generation of a general expression for the thickness of attenuating metal for a typical source located at any point in the heat exchanger. However, the absorber factor can be found by writing an expression for the attenuation of a point source located on one of the segments, summing this up over the circumference of the tube, and then summing up for all the tubes in a vertical column. This was done for the various conditions encountered such as: the heat exchanger full of flush and coolant salt with a heater, and the empty heat exchanger with and without a heater.

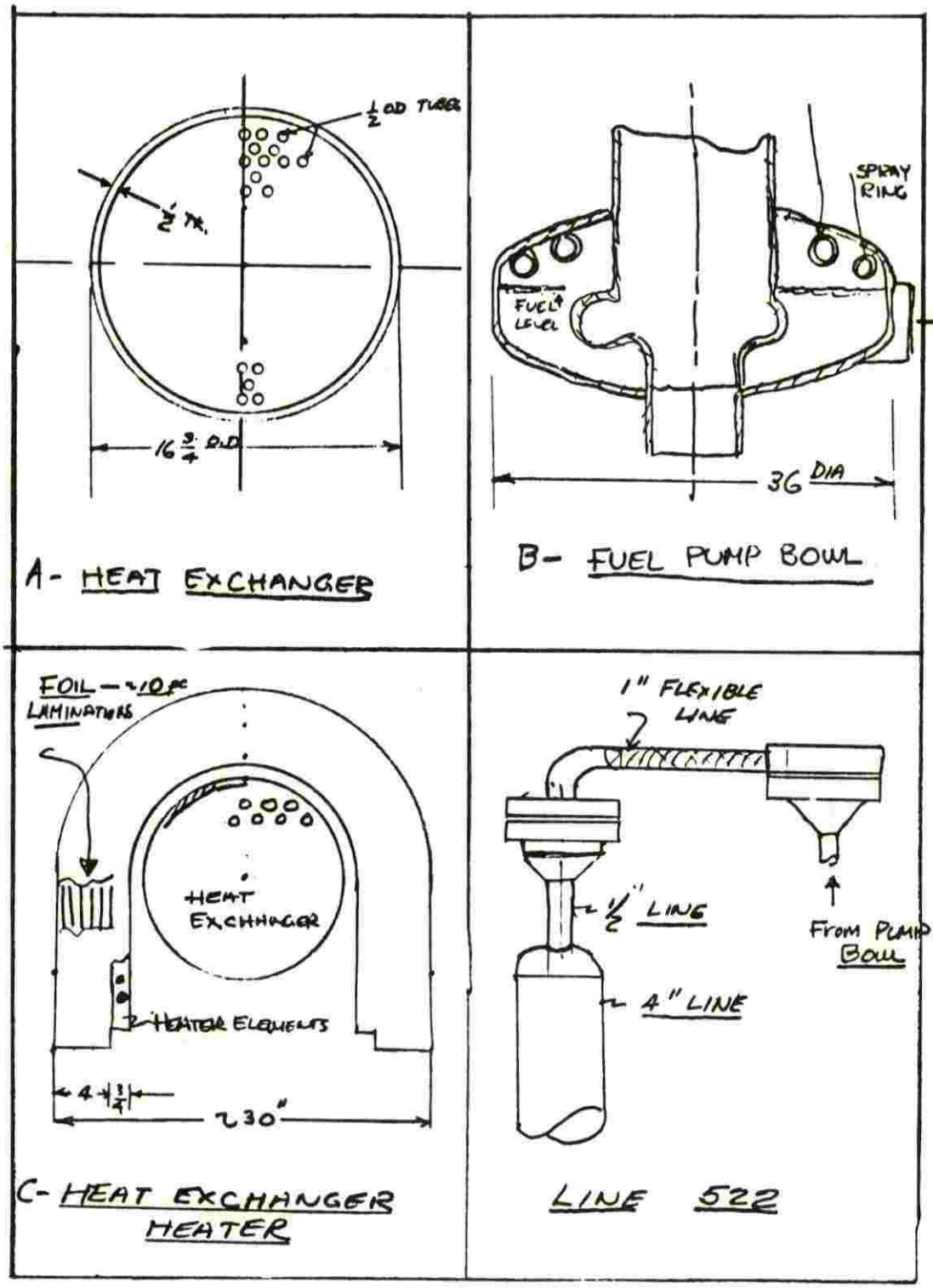

Fig. 6. Sketches of MSRE Components Scanned.

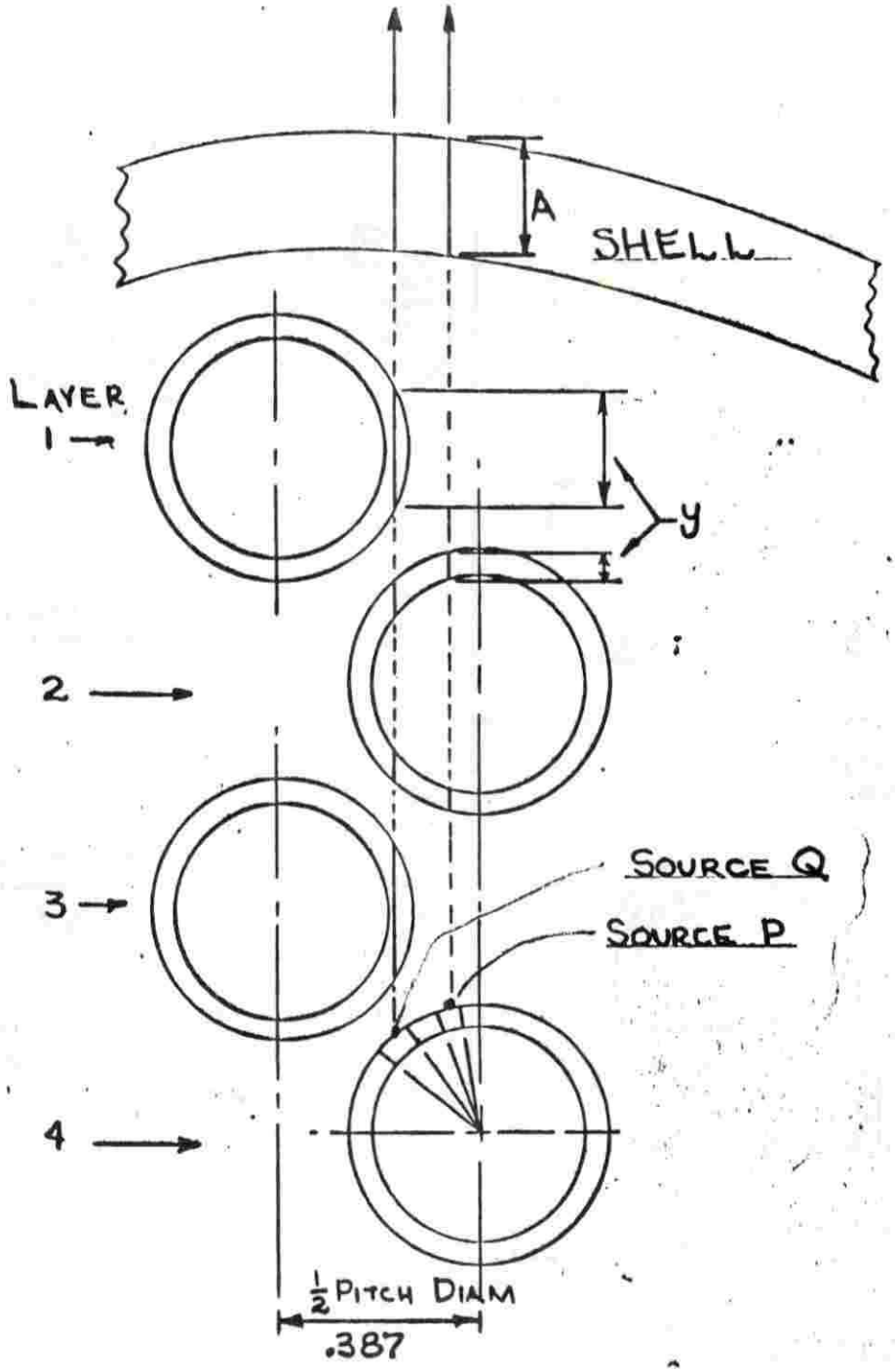

Fig. 7. Absorber Configuration in the Heat Exchanger.

1. R. L. Heath, Scintillation Spectrometer, Gamma Ray Spectrum Catalog, 2nd Ed., Vol. I, IDO Report 16880-1, August, 1964.

APPENDIX II

The tabulations and plots in this section are intended to provide data for the meaningful resolution of fission product behavior in molten salt systems. Table V gives the data for the heat exchanger and Table VI gives the data for the pump bowl and the pipe lines. So that the information will be most amenable to further interpretation and refinement, two numbers are presented for each isotope found in a given spectrum. On the same horizontal line as the spectrum number and beneath the particular isotope is the count rate corrected for only decay to the time of shutdown. Immediately below is the result calculated from Eq. 1 on page 9 in curies per sq. in. of metal surface. The reactor location of each spectrum number may be found on the plots of the heat exchanger and the pump bowl, Figures 8 through 13. Spectrum identification numbers are given in parentheses on the heat exchanger plots.

In Figures 8 through 12, calculated results in curies per sq. in. of metal are given, followed by the spectrum number inside the parentheses.

TABLE V. HEAT EXCHANGER RESULTS AND DATA

		Half life	77.7h	77.7h	66.7h	35d	39.5d	40.2h
		Energykev	230	670	740	765	497	1596
		Abundance	0.95	1.18	0.12	1.0	0.88	1.09
		Eff.Factor	1.82×10^{-10}	4.65×10^{-11}	4.1×10^{-11}	3.9×10^{-11}	6.7×10^{-11}	
Spectra	Condition of System		^{132}Te	^{132}I	^{99}Mo	^{95}Nb	^{103}Ru	^{140}La
1	Heater	Count Rate	3.67	2.13	2.05	4.70	3.65	
	+	Result	3.47	0.92	8.80	2.36	2.17	
2	Flush	Count Rate	3.93	2.64	2.74	4.41	4.14	
	Salt	Result	3.66	1.14	11.7	2.21	2.44	
3		Count Rate	0.71	2.30	1.74	3.88	3.40	
		etc.	0.67	0.99	7.45	1.94	2.02	
4			1.53	--	--	--	2.28	
			1.46	--	--	--	1.35	
8			2.84	--	--	--	--	
			3.17	--	--	--	--	
10			1.27	3.45	1.148	4.85	1.95	
			1.42	1.66	4.95	2.46	1.30	
11			0.78	1.44	0.66	2.62	1.00	
			1.98	1.28	5.53	2.64	1.26	
12			1.35	2.66	1.04	3.80	1.39	
			1.75	1.45	5.75	2.41	1.05	
13			1.15	2.41	0.61	3.90	1.41	
			1.29	1.16	2.62	1.98	0.94	
14			2.02	2.70	1.09	3.24	1.27	
			2.49	1.41	5.11	1.83	0.92	
15			2.25	--	0.56	3.50	1.32	
			2.91	--	3.12	2.22	1.00	
16			0.58	2.18	0.82	3.88	1.79	
			0.56	0.94	3.50	1.95	1.06	
17			2.00	2.81	1.24	3.41	2.26	
			2.04	1.35	5.34	1.73	1.50	
18			--	2.33	1.61	3.73	1.83	0.06
				1.12	6.94	1.89	1.22	0.047
20			--	39.92	4.35	8.76	7.26	
	No Heater		--	3.71	4.24	1.02	0.80	
22	No Flush		--	25.10	--	8.49	5.01	
	Salt		--	2.82	--	1.32	0.76	
23			11.4	41.48	3.44	13.10	7.30	
			0.87	3.37	2.89	1.37	0.71	

TABLE V. HEAT EXCHANGER RESULTS AND DATA

		Half life	77.7h	77.7h	66.7h	35d	39.5d	40.2h
		Energy kev	230	670	740	765	497	1596
		Abundance	0.95	1.18	0.12	1.0	0.88	1.09
		Eff.Factor	1.82×10^{-10}	4.65×10^{-11}	4.1×10^{-11}	3.9×10^{-11}	6.7×10^{-11}	
Spectra	Condition of System		^{132}Te	^{132}I	^{99}Mo	^{95}Nb	^{103}Ru	^{140}La
24	No Heater	Count Rate	10.02	32.09	3.12	15.08	7.78	
	No Flush	Result	0.62	2.26	2.27	1.37	0.64	
25	Salt	Count Rate	10.41	29.32	3.09	16.96	4.85	
			0.64	2.06	2.26	1.54	0.40	
26			11.14	34.64	3.10	11.45	5.73	
			0.77	2.60	2.40	1.09	0.51	
27			33.46	84.06	12.25	22.25	26.58	
			2.09	5.95	9.13	2.03	2.22	
28			30.25	86.29	12.4	22.90	25.17	
			1.95	6.18	9.20	2.11	2.13	
29			--	17.31	2.41	4.64	3.20	
				5.34	7.43	1.75	1.27	
30			--	4.84	1.59	3.77	1.54	
				0.99	3.28	0.95	0.39	
31			7.74	15.30	0.63	11.32	3.45	
			0.59	1.24	0.53	1.18	0.33	
32			13.18	20.70	2.50	14.47	4.14	
			0.80	1.46	1.83	1.31	0.34	
33			5.16	16.43	0.93	12.00	2.79	
			0.46	1.53	0.91	1.40	0.31	
35			--	21.16	--	15.49	4.28	0.21
				1.49	--	1.40	0.35	0.034
36				4.67	0.73	4.04	1.40	
				1.44	2.26	1.53	0.55	
37			16.27	39.48	4.33	17.41	10.19	
			0.99	2.78	3.17	1.57	0.83	
38				40.53	--	17.41	11.64	
				2.85	--	1.57	0.95	
73				22.38		14.11	0.75	
				4.57		3.56	0.19	
74				24.57		13.27	11.04	
				1.73		1.20	0.90	
75				23.13		12.40	9.24	0.19
				1.63		1.12	0.76	0.029

TABLE V HEAT EXCHANGER RESULTS AND DATA

		^{132}Te	^{132}I	^{99}Mo	^{95}Nb	^{103}Ru	^{140}La
Half life		77.7h	77.7h	66.7h	35d	39.5d	40.2h
Energy kev		230	670	740	765	497	1596
Abundance		0.95	1.18	0.12	1.0	0.88	1.09
Eff.Factor		1.82×10^{-10}	4.65×10^{-11}	4.1×10^{-11}	3.9×10^{-11}	6.7×10^{-11}	
Spectra	Condition of System						
76		Count Rate	13.59		13.85	9.37	
		Result	1.26		1.62	1.03	
77			--		0.27	0.12	
			--		0.03	0.013	
78			--		--	--	
					--	--	
79			18.31		14.39	7.98	
			1.30		1.32	0.67	
80			7.28		12.26	3.55	
			0.51		1.11	0.29	
81			11.48		--	2.72	.07
			0.81		--	0.22	.011
84			--		--	6.35	.266
			--		--	0.52	.041
85			24.63		12.97	8.60	
			1.85		1.24	0.76	
86	No Heater		20.50		12.24	9.39	
			4.19		3.09	2.39	
91			?		13.27	6.56	
			?		1.98	0.99	
92	With Heater		2.33		13.82	6.46	.087
	No Salt		0.28		2.06	0.97	.022
94			19.56		8.65	9.49	
			2.33		1.29	1.43	
95			5.98		6.04	4.39	
			3.15		4.26	2.46	
96			3.13		--	--	
			1.65		--	--	
97			8.74		12.48	6.03	
			1.04		1.86	0.91	
99						1.89	.052
						0.28	.013

TABLE VI

MSRE PUMP BOWL, LINES. RESULTS AND DATA

Spectra Number	Equipment		Te-132	I-132	Mo-99	Nb-95	Ru-103	La-140	Ce-141	I-131	Cs-137	Ru-106
34	L-102	Count Rate		1.45		15.49	0.37					
		Result		0.76		1.40	0.20					
39	L-102		10.41	3.48	0.91	1.76	0.96					
			3.21	1.83	5.30	1.24	0.55					
50	Pump Bowl			10.34	4.78	1.86	23.68					
				5.75	27.83	1.36	13.74					
51	"			15.85	5.24	1.40	29.30					
				8.81	30.47	1.03	17.00					
53	L-101			.99	--	3.58	0.213					
				.52	--	2.52	0.12					
54	L-102			4.69	3.15	1.04	2.60					
				2.47	18.30	0.73	1.46					
61	Pump Bowl			9.05	3.95	1.43	16.82					0.48
				0.51	23.00	1.06	9.76					1.51
62	"			28.06	10.18	1.75	61.99					1.57
				15.60	59.25	1.28	35.97					4.92
64	"		12.81	11.94	--	0.52	7.39					--
			4.16	6.64	--	0.39	4.29					--
65	"			17.98	7.45	1.15	35.20					2.72
				10.00	43.38	0.85	20.43					8.52
66	"			21.17	7.82	1.23	36.12	0.54				--
				11.77	45.52	0.90	20.96	0.78				--
67	L-522			--	4.39	0.42	19.28	0.056		2.46	2.65	0.58
				--	28.61	0.34	11.19	0.104		0.95	2.24	1.83
68	"			--	5.56	0.30	15.40	0.39	1.22	3.33	3.04	0.47
				--	36.24	0.247	8.93	0.73	0.33	1.29	2.57	1.48
69	"			--	4.41	--	16.49	1.77				
				--	28.76	--	9.57	3.28				
72	L-102			2.37		1.46	1.04					
				1.25		1.03	0.58					

Table VI - MSRE Pump Bowl, Lines. Results and Data (continuation)

Spectra Number	Equipment		Te-132	I-132	Mo-99	Nb-95	Ru-103	La-140	Ce-141	I-131	Cs-137	Ru-106
82	L-102			1.12		0.69	0.41					
				0.587		0.489	0.23					
93	L-102			13.36		7.71	10.28					
				7.04		5.43	5.76					
95	HX Inlet	Count Rate		5.98		6.04	4.39					
		Result		3.15		4.26	2.46					
96	L-102	Count Rate		3.13		1.12	1.18					
		Result		1.65		0.785	0.66					

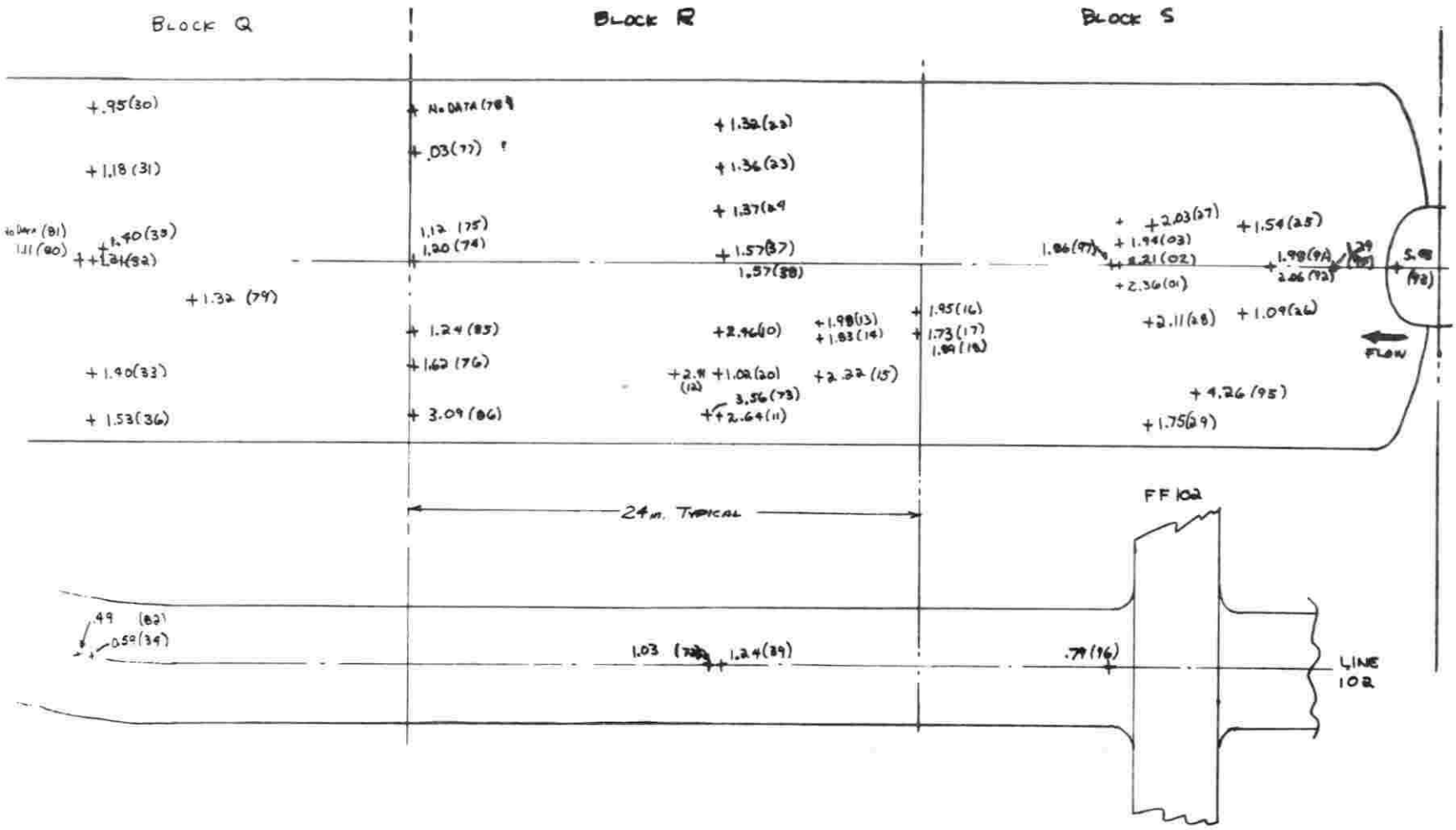

Fig. 8. Heat Exchanger Plot for ^{95}Nb.

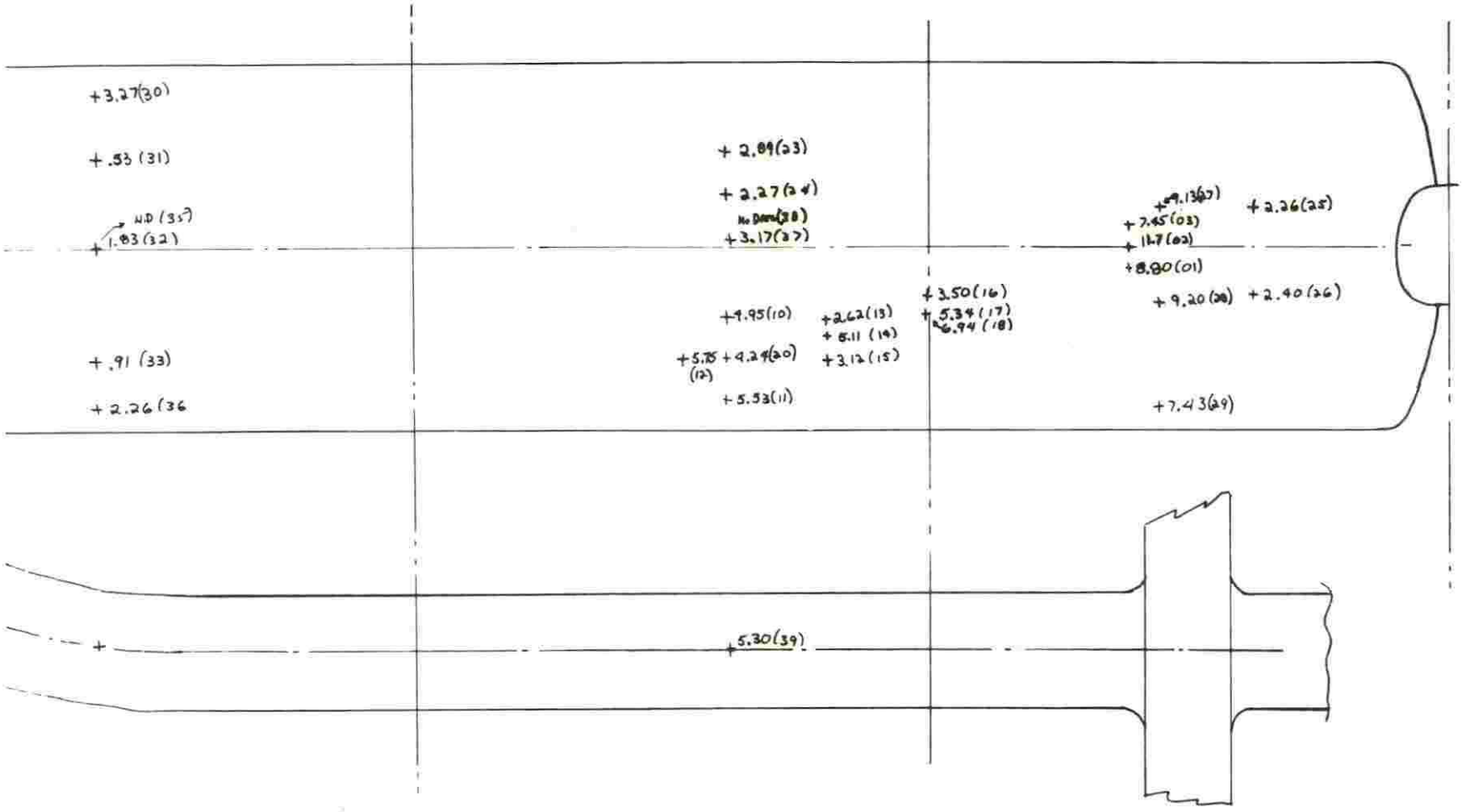

Fig. 9. Heat Exchanger Plot for ^{99}Mo.

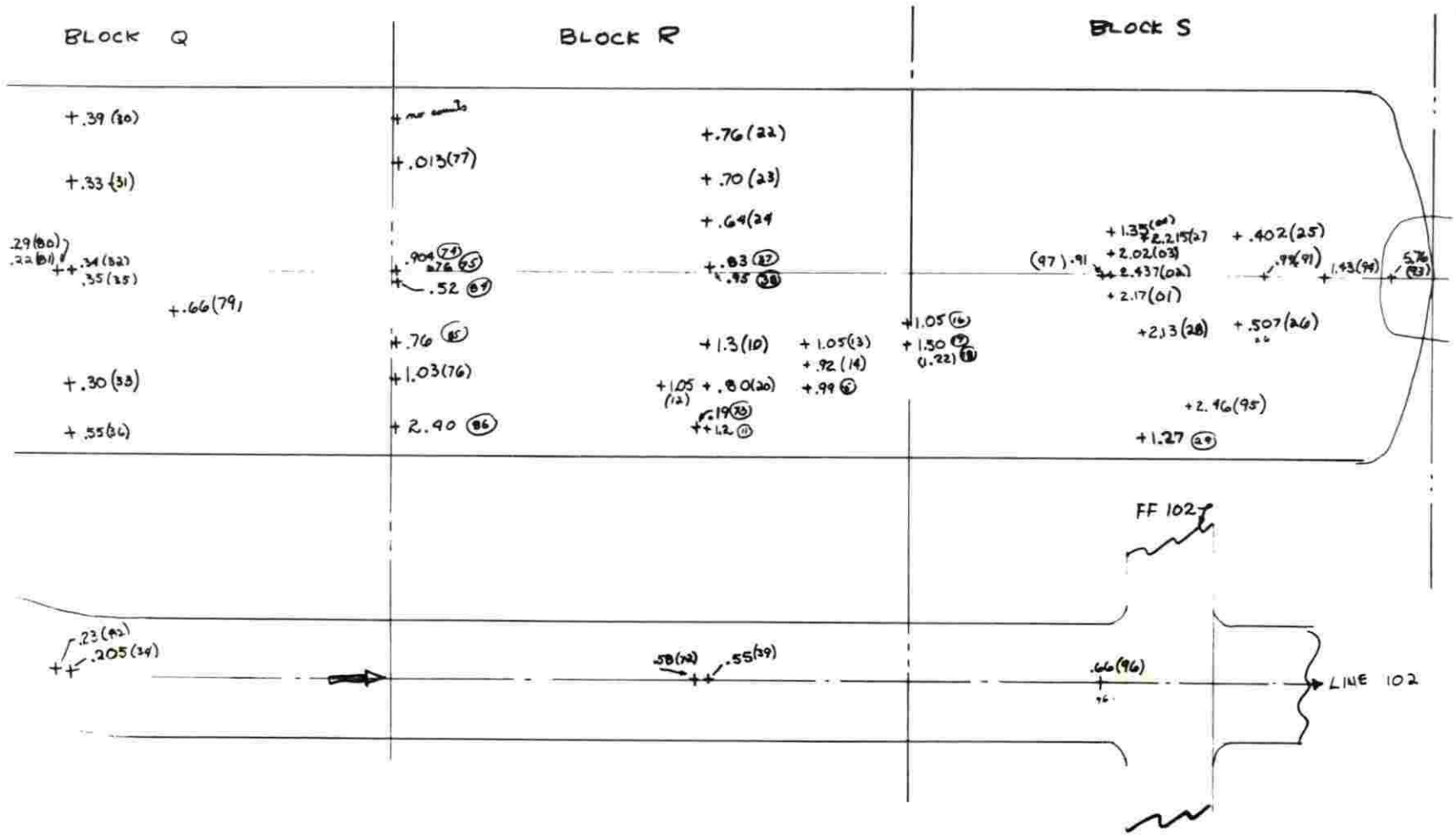

Fig. 10. Heat Exchanger Plot for ^{103}Ru.

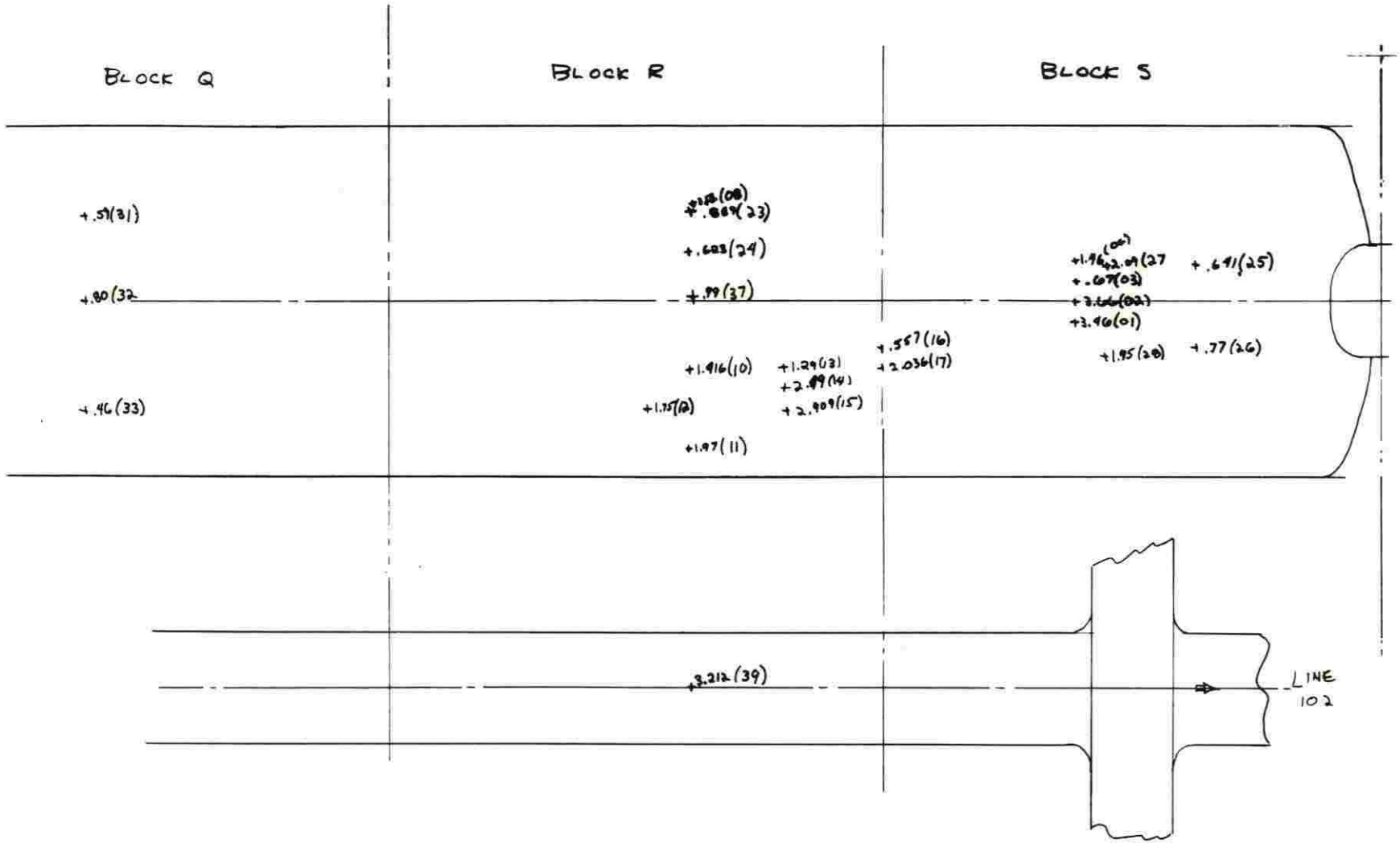

Fig. 11. Heat Exchanger Plot for ^{132}Te.

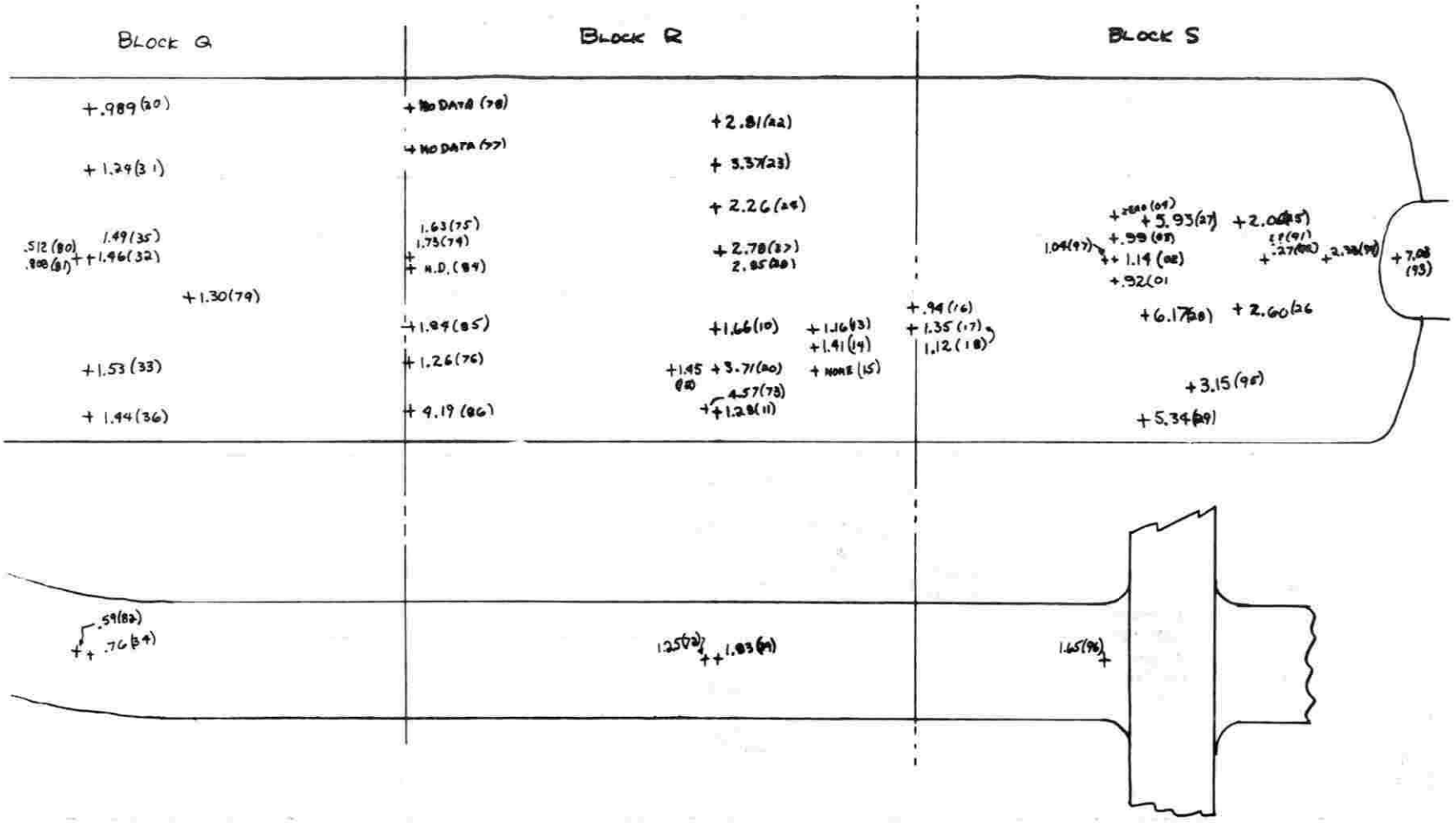

Fig. 12. Heat Exchanger Plot for ^{132}I.

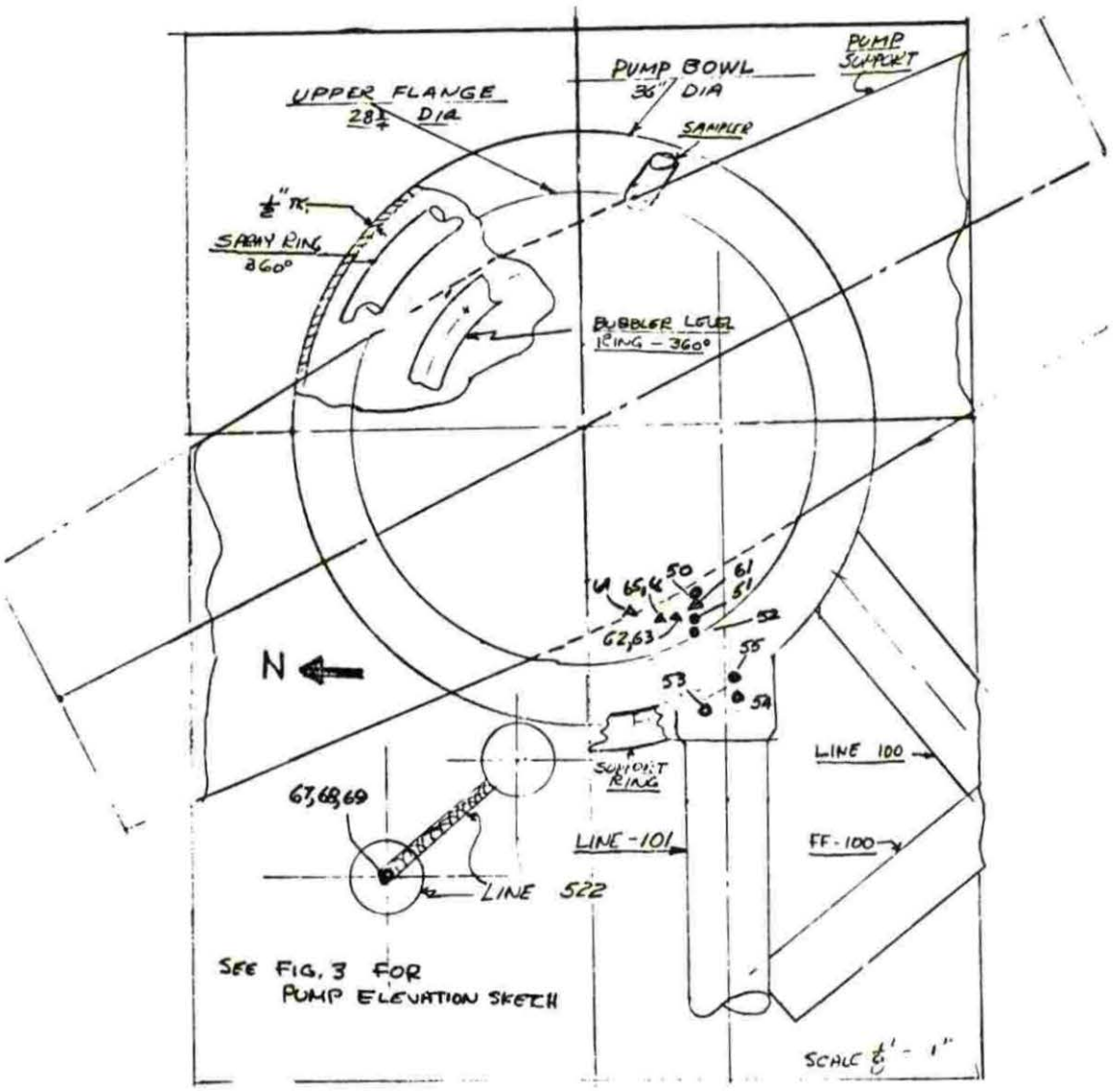

Fig. 13. Pump Bowl Area Showing Line 522 Pump Support and Internals with Scan Locations.